

# Specific heat and quantized thermal conductance of single-walled boron nitride nanotubes

Y. Xiao,<sup>1</sup> X. H. Yan,<sup>1,2,\*</sup> J. X. Cao,<sup>1</sup> J. W. Ding,<sup>1</sup> Y. L. Mao,<sup>1</sup> and J. Xiang<sup>1</sup>

<sup>1</sup>*Department of Physics & Institute of Modern Physics, Xiangtan University, Xiangtan 411105, Hunan, China*

<sup>2</sup>*Interdisciplinary Center of Theoretical Studies and Institute of Theoretical Physics, CAS, Beijing 10080, China*

(Received 31 August 2003; revised manuscript received 7 January 2004; published 28 May 2004)

The thermal properties of single-walled boron nitride nanotubes are calculated. It is found that boron nitride nanotubes have a larger specific heat than that of carbon nanotubes. The fitting formulas for diameter and chirality dependence of specific heat at 300 K are given. Moreover, thermal conductance of single-walled boron nitride nanotubes exhibits a universal quantization at low temperature, which is independent of the diameter and chirality of nanotubes.

DOI: 10.1103/PhysRevB.69.205415

PACS number(s): 61.46.+w, 65.80.+n, 63.22.+m, 78.30.-j

Following the discovery<sup>1</sup> and extensive research<sup>2-8</sup> of carbon nanotubes (CNT's), its derivative boron nitride nanotubes (BNNT's) have attracted considerable attention in recent years due to anticipated exciting properties.<sup>9,10</sup> It has been reported that BNNT's have remarkable mechanical properties. For example, the axial Young's modulus of multiwalled BNNT's has been measured to be 1.22 TPa.<sup>11</sup> Contrary to the dependence of the band structure to the geometrical structure of CNT's, the energy gap of BNNT's is about 5 eV,<sup>12,13</sup> which seems to be independent of wall numbers, diameter, or chirality. These results signify more practical applications of BNNT's in nanosized electronic and photonic devices than those of CNT's. However, excellent thermal transport management is indispensable in the design and performances of modern microelectronic devices.<sup>14,15</sup> So, it is necessary to theoretically reveal the essential relationship between the unique structures and the special thermal properties of BNNT's.

It is an effective avenue to investigate phonon structure for the study of thermal properties of BNNT's. Series of calculations of phonon in BNNT's have been performed using tight-binding model,<sup>16</sup> density-functional theory,<sup>17</sup> and valence shell model.<sup>18</sup> Of these, the valence shell model provides an intuitive understanding of phonon based on force constants fitted to the phonon dispersion of monolayer of hexagonal boron nitride (h-BN).<sup>19</sup> However, the quadratic wave-vector dependence of the frequency for out-of-plane phonons of two-dimensional (2D) h-BN cannot be produced. Wirtz *et al.* have calculated phonon-dispersion relations (PDR) of BNNT's by virtue of density-functional theory. Since large computational demands are required, it may be difficult to calculate the phonon in BNNT's with large atoms in the unit cell. Here we use a force-constant model combined with the consideration of symmetry of nanotubes to calculate phonon in BNNT's.<sup>20-24</sup> The best-fit parameters are obtained in Table I. In this model, it is crucial to determine the force constants between two atoms. In order to get the reasonable out-of-plane phonons, up to the fourth nearest-neighbor interactions for 2D h-BN are introduced.

The phonon spectrum of 2D h-BN is calculated as shown in Fig. 1(a), in which the available experimental points are included.<sup>19</sup> Compared with those of valence shell model, our results reproduce the experimental data very well along the  $\Gamma-K$  direction. It does mean that the model is reasonable

and parameters listed in Table I are reliable. The PDR of (10, 10) BNNT is shown in Fig. 1(b). Around  $\Gamma$  point, there are four acoustic modes: one longitudinal (LA), two degenerate transverse (TA), and one twisting (WA), all of which have linear dispersion at low energy. The sound velocities of TA, WA, and LA modes for a (10, 10) BNNT are estimated as 8.73, 12.85, and 17.17 km/s, respectively. The high sound velocity, combined with the small diameter of nanotubes, causes the relatively large subband splitting. Such a splitting would have an important influence on the specific heat. In comparison with other phonon modes, the radial breathing mode (RBM) is known to have strong Raman intensities in low-frequency regions,<sup>25-27</sup> which can be used to characterize the BNNT's samples. It is found that the frequency of RBM of BNNT's is inversely proportional to the radius, i.e.,  $\omega_{RBM} = A/r$  with  $A = 951 \text{ cm}^{-1} \text{ \AA}$ . The value of  $A$  is nearly consistent with that in Refs. 16 and 17.

As PDR is determined, vibrational density of states (VDOS) can be written as

$$g(\omega) = \frac{\Omega}{(2\pi)^3} \int \frac{dS}{|\nabla_q \omega(q)|} = \frac{\Omega}{(2\pi)^3} \sum_q \frac{\delta}{(\omega - \omega_q)^2 + \delta^2}, \quad (1)$$

where  $\delta$  is adjustable width factor of Lorentzian function. In term of VDOS, specific heat  $C_V$  at temperature  $T$  is then given by the formula

$$C_V(T) = \int_0^{w_{\max}} k_B \left( \frac{\hbar \omega}{k_B T} \right)^2 \frac{\exp(\hbar \omega / k_B T)}{[\exp(\hbar \omega / k_B T) - 1]^2} g(\omega) d\omega, \quad (2)$$

TABLE I. Force-constant parameters for 2D h-BN in units of  $10^4 \text{ dyn/cm}$ . Here the subscripts  $r$ ,  $ti$ , and  $to$  refer to radial, transverse in plane, and transverse out of plane, respectively.

Radial	Tangential	
$\phi_r^{(1)} = 31.00$	$\phi_{ti}^{(1)} = 18.50$	$\phi_{to}^{(1)} = 5.60$
$\phi_r^{(B-B)} = 7.00$	$\phi_{ti}^{(B-B)} = -3.23$	$\phi_{to}^{(B-B)} = -0.70$
$\phi_r^{(N-N)} = 8.00$	$\phi_{ti}^{(N-N)} = -0.73$	$\phi_{to}^{(N-N)} = -0.55$
$\phi_r^{(3)} = 1.00$	$\phi_{ti}^{(3)} = -3.25$	$\phi_{to}^{(3)} = 0.65$
$\phi_r^{(4)} = -1.90$	$\phi_{ti}^{(4)} = 1.29$	$\phi_{to}^{(4)} = -0.30$

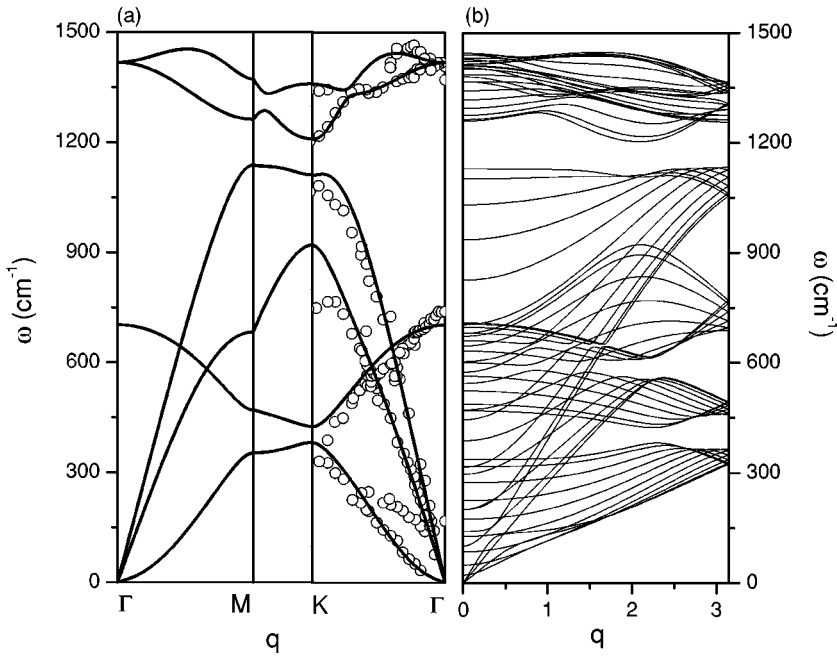


FIG. 1. Phonon dispersion relation (a) for 2D h-BN and (b) for (10, 10) BNNT.

where  $\hbar$  and  $k_B$  are the Planck constant and the Boltzmann constant, respectively. The calculated specific heat of (10, 10) BNNT is shown in Fig. 2(a), together with a comparison to that of (10, 10) CNT. When temperature is very low, the specific heat increases linearly with the increase of temperature [see the inset of Fig. 2(a)]. This is because only acoustic phonons are populated. For temperatures larger than 6 K, however, the slope of the curve increases due to the populations of optical phonons, which is expected to be the signature of one-dimensional (1D) quantized phonon spectrum in single-walled BNNT's. In addition, the specific heat of (10, 10) BNNT is larger than that of (10, 10) CNT. The relation between specific heat and thermal conductivity satisfies  $\kappa = \sum C_v v l$ , where  $v$  and  $l$  are the phonon group velocity and the phonon mean-free path. At low temperature, the Um-

klapp scattering freezes out and the phonon mean-free path  $l$  is constant with temperature.<sup>14,15,28-30</sup> So one may suppose that thermal conductivity follows the temperature dependence of specific heat. Assuming BNNT's have the same  $l$  as CNT's, BNNT's would have a larger low-temperature thermal conductivity than CNT's. Such a phenomenon shows that BNNT may provide another candidate for thermal management in molecular electronics.

Figure 2(b) shows the specific heat for 2D h-BN, (10, 10) and (10, 0) BNNT's, as well as experimental data of 3D h-BN.<sup>31</sup> One finds that 2D h-BN has a larger specific heat than 3D h-BN below 60 K, a consequence of interlayer coupling in 3D h-BN. Compared with 2D h-BN, the (10, 10) and (10, 0) BNNT's have a smaller specific heat below about 200 K. Moreover, the specific heat curve of (10, 0) BNNT lies

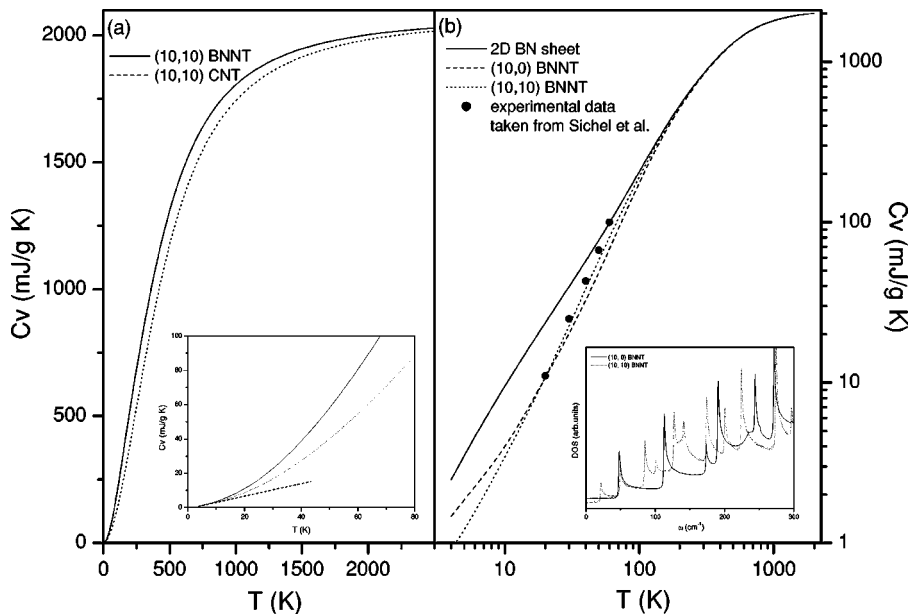


FIG. 2. (a) Specific heat of (10, 10) BNNT and CNT. (b) Temperature dependence of specific heat of BNNT's and 2D h-BN.

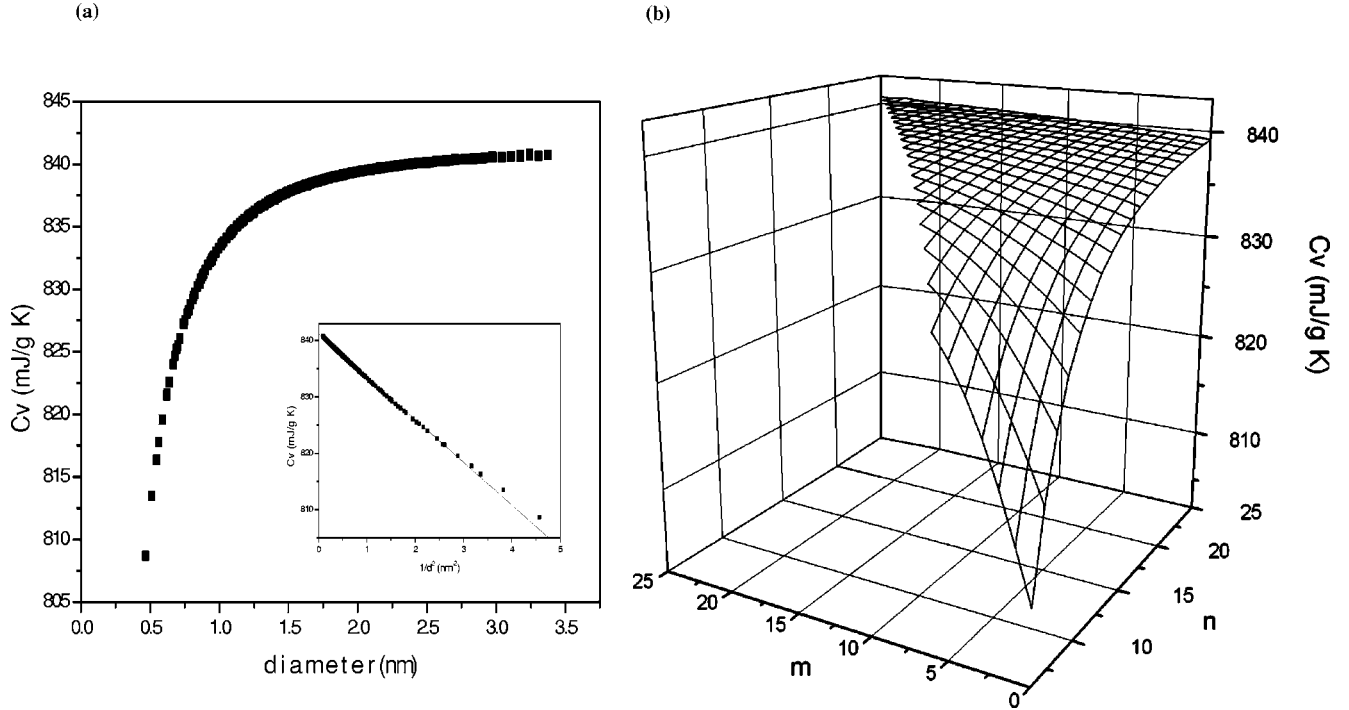


FIG. 3. Specific heat of BNNT's at 300 K as a function of tube diameter (a) and tube indices (b).

well above that of (10, 10) BNNT at low temperature. This behavior is attributed to the fact that VDOS of (10, 0) BNNT is larger than that of (10, 10) BNNT at low energy. If  $\omega_0$  is the frequency of the first optical phonon, the optical phonon will give negligible contribution to specific heat for temperature lower than  $T_0 \approx \hbar \omega_0 / k_B$ , with  $T_0 = 31$  K for (10, 10) tube and  $T_0 = 70.6$  K for (10, 0) tube. With the increase of temperature ( $T > T_0$ ), the first optical phonon with  $\omega_0 = 21.5 \text{ cm}^{-1}$  for (10, 10) BNNT would be activated and contribute to the specific heat, which results in a higher specific heat than that of (10, 0) BNNT. As temperature increases further, the specific heat curve of (10, 10) BNNT lies well above that of (10, 0) BNNT. Above 200 K, specific heat curves of (10, 10) and (10, 0) BNNT's follow the 2D h-BN curve. Consequently, the low-temperature specific heat directly presents quantized phonon subbands in BNNT's, and reflects the dimensionality of boron nitride systems.

The diameter and chirality dependence of specific heat at 300 K for  $(n, m)$  BNNT's ( $n = 6-25, m = 0-n$ ) are shown in Fig. 3. As shown in Fig. 3 (a), the specific heat increases rapidly with increasing diameter for small-diameter BNNT's. However, the specific heat of large-diameter BNNT's would approach the value of  $C_{v2D} = 841 \text{ mJ/g K}$  ( $C_{v2D}$  is the specific heat of 2D h-BN at 300 K). From the inset, one can see that the specific heat is linear with  $d^{-2}$  with the diameter  $d$ . The best-fit formula can be given as

$$C_v = C_{v2D} - 7.6/d^2. \quad (3)$$

This fitting is in agreement with calculated results for large diameter BNNT's, while a small deviation from the calculated results occurs for small diameter BNNT's. The deviation may be attributed to the curvature effect of small diameter nanotubes. From Eq. (3), one can see that  $C_v \rightarrow C_{v2D}$  as

$d \rightarrow \infty$ . Such a phenomenon could be explained by the fact that BNNT's with large enough diameter can be thought of as a h-BN sheet with periodic boundary conditions imposed in the circumferential direction.<sup>32</sup> It is found that the chirality dependence of specific heat is similar to the diameter dependence. It is easy to fit the specific heat at 300 K in  $(n, m)$  BNNT by

$$C_v = C_{v2D} - \frac{B}{d^2} \left[ 240.0 + 57.3 \arctan \left( \frac{\sqrt{3}m}{2n+m} \right) \right] \quad (4)$$

with  $B = 0.03 \text{ mJ/g K nm}^2/\text{deg}$ . Due to chiral angle  $\theta = 57.3 \arctan(\sqrt{3}m/2n+m)$  (deg), Eq. (8) is simplified to  $C_v = C_{v2D} - (B/d^2)[240.0 + \theta]$ .

From Fig. 3(b), one can see that specific heat increases with index  $m$  for  $(n, m)$  BNNT's with fixed  $n$ . The chirality dependence of specific heat of BNNT's has an analogy to that of energy gap for CNT's,<sup>8</sup> which may suggest that both electrical and thermal properties of nanotubes is closely related to their geometrical structures. Due to the difficulty of production of nanotubes with specific indices  $n, m$ , Eq. (4) is important to evaluate qualitatively the specific heat of samples with a diameter distribution. Moreover, recent experiment has shown that the phonon-drag effect plays an important role in deciding the thermopower of CNT's.<sup>33</sup> The magnitude of the phonon-drag contribution to thermopower depends mainly on their specific heat. Consequently, it is expected that Eqs. (3) and (4) may be applicable for evaluating the specific heat in a thermoelectric energy conversion circuit.

Based on Landauer formulation of transport theory, it is possible to obtain the thermal conductance of BNNT's. As-

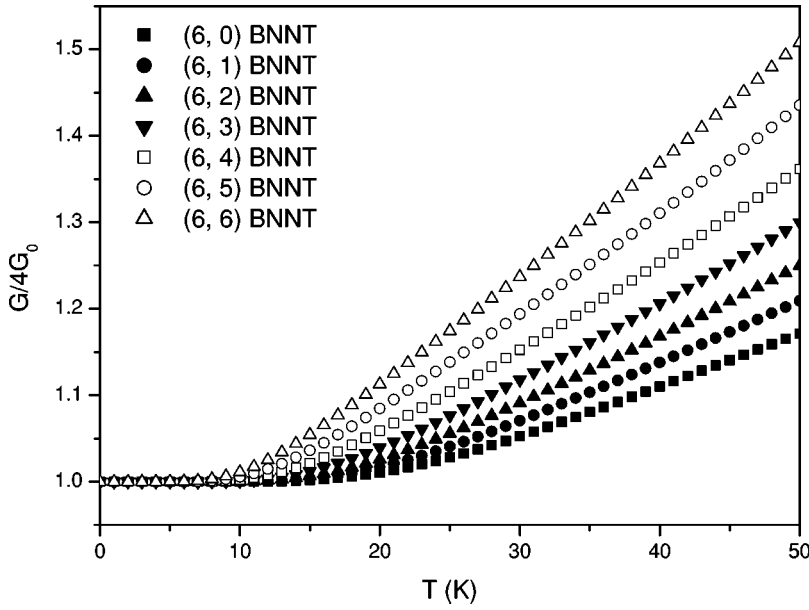


FIG. 4. Thermal conductance for  $(6,m)$  BNNT's ( $m=0-6$ ) at low temperature.

suming perfectly adiabatic contact between the thermal reservoirs and BNNT's, thermal conductance is given by the formula<sup>34,35</sup>

$$G = \frac{k_B^2 T}{h} \sum_m \int_{\omega_m^{\min}}^{\omega_m^{\max}} dx \frac{x^2 e^x}{(e^x - 1)^2}, \quad (5)$$

where  $x_m = \hbar \omega_m / k_B T$ ,  $\omega_m^{\min}$ , and  $\omega_m^{\max}$  are the minimum and the maximum frequency of the  $m$ th phonon branch in PDR of BNNT's.

In Fig. 4, we calculate thermal conductance of  $(6,m)$  BNNT's ( $m=0-6$ ), normalized to  $4G_0 = 4\pi^2 k_B^2 T / 3h$  (for reason described below). One can see that thermal conductance of BNNT's increases with the increase of tube diameter. In addition, thermal conductance of all seven BNNT's starts from a smooth value  $G = 4G_0$  at  $T < T_c$  [ $T_c = 8$  K for  $(6,6)$  BNNT], and then increase with temperature  $T$  at  $T > T_c$ . The smooth value of  $G$  suggests that phonon thermal conductance be quantized at  $T < T_c$ , which can be derived analytically from Eq. (5). Performing the integration in Eq. (5), we present an analytic form of thermal conductance

$$G = F(x_m^{\min}) - F(x_m^{\max}), \quad (6)$$

where  $F(x_m) = 2k_B^2 T / h \sum_m [(x_m^2 / 2(e^{x_m} - 1))] + \sum_{n=1}^{\infty} [(e^{-nx_m} / n^2) + x_m e^{-nx_m} / n]$ . In particular, four acoustic modes with  $x_m^{\min} = 0$  contribute a universal quantum of  $4F(x_m^{\min}) = 4\pi^2 k_B^2 T / 3h = 4G_0$  to thermal conductance. This indicates that thermal conductance of BNNT's increases linearly with temperature at low temperature, which has an analogy to the experimental results of thermal conductivity of single-walled CNT's samples.<sup>28</sup> From a conventional point of view,<sup>36</sup> the phonon mean-free path  $l$  is independent of temperature and

specific heat is proportional to temperature at low temperature. Consequently, temperature dependence of thermal conductivity of BNNT's would be almost linear at low temperature. Moreover, the value of  $T_c$  decreases with increasing diameter. This result is attributed to the population of the first optical phonon mode  $E_2$ , which decreases with increasing diameter. The first optical phonon mode plays an important role in both specific heat and thermal conductance, which reveals the underlying quantized phonon spectrum of BNNT's. Additionally, quantized thermal conductance has been observed experimentally and predicted theoretically,<sup>34,35,37</sup> which provides an insight into the quantum physics in nanotube-based devices.

In summary, we have investigated the specific heat of BNNT's based on a force-constant model within lattice-dynamics theory. The results show that the specific heat of BNNT's decreases linearly with decreasing temperature at low temperature. We predict a higher thermal conductivity for BNNT's than that for CNT's. The diameter and chirality dependence of specific heat at 300 K are fitted for all types of BNNT's. The present results are important for the correct evaluation of specific heat of BNNT's suggested for thermal transport and thermoelectric energy conversion applications. Moreover, it is found that thermal conductance of BNNT's exhibits a universal quantization at low temperature, independent of diameter and chirality of nanotubes.

This work was supported by National Major Project of China (Grant No. 1999-0645-4500) and the Project Supported by Scientific Research Fund of Hunan Provincial Education Department (Grant Nos. 03A046 and 03JZY3019), and partly by the Science & Technology Foundation for Ministry of Education (Grant Nos. 204099 and 03JJY3010).

\*Corresponding author. Email address: xhyan@xtu.edu.cn

<sup>1</sup>S. Iijima, *Nature (London)* **354**, 56 (1991); S. Iijima and T. Ichihashi, *ibid.* **363**, 603 (1993); D.S. Bethune, C.-H. Kiang, M.S.

de Vries, G. Gorman, R. Savoy, J. Vazquez, and R. Beyers, *ibid.* **363**, 605 (1993).

<sup>2</sup>M. S. Dresselhaus, G. Dresselhaus, and P. C. Eklund, *Science of*

- Fullerenes and Carbon Nanotubes* (Academic, San Diego, 1996).
- <sup>3</sup>R. Saito, G. Dresselhaus, and M. S. Dresselhaus, *Physical Properties of Carbon Nanotubes* (Imperial College Press, London, 1998).
  - <sup>4</sup>J. Hone, B. Batlogg, Z. Benes, A.T. Johnson, and J.E. Fischer, *Science* **289**, 1730 (2000).
  - <sup>5</sup>G. Chen, S. Bandow, E.R. Margine, C. Nisoli, A.N. Kolmogorov, V.H. Crespi, R. Gupta, G.U. Sumanasekera, S. Iijima, and P.C. Eklund, *Phys. Rev. Lett.* **90**, 257403 (2003).
  - <sup>6</sup>R. Akdim, R. Pachter, X.F. Duan, and W.W. Adams, *Phys. Rev. B* **67**, 245404 (2003).
  - <sup>7</sup>D. Sanchez-Portal, E. Artacho, J.M. Soler, A. Rubio, and P. Ordejon, *Phys. Rev. B* **59**, 12 678 (1999).
  - <sup>8</sup>J.W. Ding, X.H. Yan, and J.X. Cao, *Phys. Rev. B* **66**, 073401 (2002).
  - <sup>9</sup>N.G. Chopra, R.J. Luyken, K. Cherrey, V.H. Crespi, M.L. Cohen, S.G. Louie, and A. Zettl, *Science* **266**, 966 (1995).
  - <sup>10</sup>E. Hernandez, C. Goze, P. Bernier, and A. Rubio, *Phys. Rev. Lett.* **80**, 4502 (1998).
  - <sup>11</sup>N.G. Chopra and A. Zettl, *Solid State Commun.* **105**, 297 (1998).
  - <sup>12</sup>A. Rubio, J.L. Corkill, and M.L. Cohen, *Phys. Rev. B* **49**, 5081 (1994).
  - <sup>13</sup>X. Blase, A. Rubio, S.G. Louie, and M.L. Cohen, *Europhys. Lett.* **28**, 3085 (1994).
  - <sup>14</sup>P. Kim, L. Shi, A. Majumdar, and P.L. McEuen, *Phys. Rev. Lett.* **87**, 215502 (2001).
  - <sup>15</sup>S. Berber, Y.K. Kwon, and D. Tomanek, *Phys. Rev. Lett.* **84**, 4613 (2000).
  - <sup>16</sup>D. Sanchez-Portal and E. Hernandez, *Phys. Rev. B* **66**, 235415 (2002).
  - <sup>17</sup>L. Wirtz, A. Rubio, R.A. de la Concha, and A. Loiseau, *Phys. Rev. B* **68**, 045425 (2003).
  - <sup>18</sup>V.N. Popov, *Phys. Rev. B* **67**, 085408 (2003).
  - <sup>19</sup>E. Rokuta, Y. Hasegawa, K. Suzuki, Y. Gamou, C. Oshima, and A. Nagashima, *Phys. Rev. Lett.* **79**, 4609 (1997).
  - <sup>20</sup>R. Saito, T. Takeya, T. Kimura, G. Dresselhaus, and M.S. Dresselhaus, *Phys. Rev. B* **57**, 4145 (1998).
  - <sup>21</sup>J.X. Cao, X.H. Yan, Y. Xiao, Y. Tang, and J.W. Ding, *Phys. Rev. B* **67**, 045413 (2003).
  - <sup>22</sup>J.X. Cao, X.H. Yan, and Y. Xiao, *J. Phys. Soc. Jpn.* **72**, 2256 (2003).
  - <sup>23</sup>V.N. Popov, V.E. Van Doren, and M. Balkanski, *Phys. Rev. B* **59**, 8355 (1999).
  - <sup>24</sup>J. Maultzsch, S. Reich, C. Thomsen, E. Dobardžić, I. Milošević, and M. Damnjanović, *Solid State Commun.* **121**, 471 (2002).
  - <sup>25</sup>A.M. Rao, E. Richter, S. Bandow, B. Chase, P.C. Eklund, K.A. Williams, S. Fang, K.R. Subbaswamy, M. Menon, A. Thess, R.E. Smalley, G. Dresselhaus, and M.S. Dresselhaus, *Science* **275**, 187 (1997).
  - <sup>26</sup>C. Thomsen and S. Reich, *Phys. Rev. Lett.* **85**, 5214 (2001).
  - <sup>27</sup>J. Kurti, G. Kresse, and H. Kuzmany, *Phys. Rev. B* **58**, R8869 (1999).
  - <sup>28</sup>J. Hone, M. Whitney, C. Piskoti, and A. Zettl, *Phys. Rev. B* **59**, R2514 (1999).
  - <sup>29</sup>J.C. Lasjaunias, K. Biljakovic, Z. Benes, J.E. Fischer, and P. Monceau, *Phys. Rev. B* **65**, 113409 (2002).
  - <sup>30</sup>Y. Xiao, X.H. Yan, J.X. Cao, and J.W. Ding, *J. Phys.: Condens. Matter* **15**, L341 (2003).
  - <sup>31</sup>E.K. Sichel, R.E. Miller, M.S. Abrahams, and C.J. Buiocchi, *Phys. Rev. B* **13**, 4607 (1976).
  - <sup>32</sup>L.X. Benedict, S.G. Louie, and M.L. Cohen, *Solid State Commun.* **100**, 177 (1996).
  - <sup>33</sup>J. Vavro, M.C. Llaguno, J.E. Fischer, S. Ramesh, R.K. Saini, L.M. Ericson, V.A. Davis, R.H. Hauge, M. Pasquali, and R.E. Smalley, *Phys. Rev. Lett.* **90**, 065503 (2003).
  - <sup>34</sup>K. Schwab, E.A. Henriksen, J.M. Worlock, and M.L. Roukes, *Nature (London)* **404**, 974 (2000).
  - <sup>35</sup>L.G.C. Rego and G. Kirczenow, *Phys. Rev. Lett.* **81**, 232 (1998).
  - <sup>36</sup>J.X. Cao, X.H. Yan, Y. Xiao, and J.W. Ding, *Phys. Rev. B* **69**, 073407 (2004).
  - <sup>37</sup>T. Yamamoto, S. Watanabe, and K. Watanabe, *Phys. Rev. Lett.* **92**, 075502 (2004).